# The Characterization of Catalyst for Internal Reforming Molten Carbonate Fuel Cell

*Chang-Sung Jun*, Seongyoun Park, Yun Sung Kim and Tae Won Lee*
*Corporate R&D Institute Doosan Heavy Industries & Construction Co., Ltd., Daejeon 305-811, Korea*
** Corresponding author (Tel:+82-42-712-2164, E-mail:changsung.jun@doosan.com)*

## Abstract

Thermal stability of the Internal Reforming Molten Carbonate Fuel Cell (IR-MCFC) stack is one of the most important variables to be controlled for long term operation. Generally, the internal reforming catalyst loading pattern can manage stack's thermal distribution because the endothermic reaction of the steam reforming can remove partially heat generated by electrochemical reaction during stack operation. Therefore, the internal reforming catalyst loading pattern has to be decided to minimize of thermal stress distribution of stack and to obtain uniform temperature distribution. The aim of this work is to study the intrinsic kinetics of stream reforming reaction, accompanied by the reverse water gas shift reaction over a commercial $Ni/Al_2O_3$ catalyst, and this performance decay rate for simulation and optimal design of IR-MCFC stack. The main reactions involved in methane steam reforming have been analyzed thermodynamically. A reaction mechanism for methane steam reforming is proposed, and kinetic rate equations have been developed by using the Langmuir-Hinshelwood approach and Freundlich's adsorption concept. The column cell type micro reactor was used to study the mechanism and the kinetics of the catalysts under wide ranges of temperature, steam to carbon ratio and pressure conditions. And the single cell test was also used to predict and verify the performances of the catalysts.

### *1. Introduction*

The Internal Reforming (IR) MCFC can control the temperature distribution of stack by using internal reforming which is endothermic reaction. And internal reforming reaction occurs in the anode gas channel with anode electrode, and the produced hydrogen directly be used to anode reaction, therefore the conversion of reforming can be over the thermodynamic equilibrium conversion. But, if we want to control the temperature distribution of stack, we need to analyze the kinetic rate equation of steam reforming.

The objective of this work is to study the intrinsic kinetics of the steam reforming reaction. The overall reaction of methane and steam to form carbon, carbon monoxide, carbon dioxide and hydrogen are presented by the equations listed in Table 1. The process of methane steam reforming and the reverse water gas shift reaction can be described on the basis of reactions 1~3 for the kinetics study.

**Table 1. Possible reactions in methane steam reforming and equilibrium constants**

| No. | Reactions | $-\triangle H_{298}$,kJ/mol | $K_{pi}$ | Dimensions |
|---|---|---|---|---|
| 1 | $CH_4 + H_2O \rightarrow CO + 3H_2$ | - 206.1 | $1.198 * 10^{17} \exp(-26830/T)$ | $(kPa)^2$ |
| 2 | $CO + H_2O \rightarrow CO_2 + H_2$ | + 41.15 | $1.767 * 10^{-2} \exp(4400/T)$ | $(kPa)^0$ |
| 3 | $CH_4 + 2H_2O \rightarrow CO_2 + 4H_2$ | - 165.0 | $2.117 * 10^{15} \exp(-22430/T)$ | $(kPa)^2$ |
| 4 | $CH_4 + CO_2 \rightarrow 2CO + 2H_2$ | - 247.3 | $6.780 * 10^{18} \exp(-31230/T)$ | $(kPa)^2$ |
| 5 | $CH_4 + 3CO_2 \rightarrow 4CO + 2H_2O$ | - 330.0 | $2.170 * 10^{22} \exp(-40030/T)$ | $(kPa)^2$ |

| | | | | |
|---|---|---|---|---|
| 6 | $CH_4 \rightarrow C + 2H_2$ | - 74.82 | $4.161 * 10^7 \exp(-10614/T)$ | kPa |
| 7 | $2CO \rightarrow C + CO_2$ | + 173.3 | $5.744 * 10^{-12} \exp(20634/T)$ | $(kPa)^{-1}$ |
| 8 | $CO + H_2 \rightarrow C + H_2O$ | + 131.3 | $3.173 * 10^{-10} \exp(16318/T)$ | $(kPa)^{-1}$ |
| 9 | $CO_2 + 2H_2 \rightarrow C + 2H_2O$ | + 90.13 | $1.753 * 10^{-8} \exp(12002/T)$ | $(kPa)^{-1}$ |
| 10 | $CH_4 + 2CO \rightarrow 3C + 2H_2O$ | + 187.6 | $4.190 * 10^{-12} \exp(22022/T)$ | $(kPa)^{-1}$ |
| 11 | $CH_4 + CO_2 \rightarrow 2C + 2H_2O$ | + 15.3 | $0.730 * \exp(1388/T)$ | $(kPa)^0$ |

A large number of reaction schemes were proposed by many researchers. On developing the kinetic mechanism, the following basic assumptions were made based on information which is well accepted in the literature.

1) $H_2O$ reacts with surface Ni atoms, yielding adsorbed oxygen and gaseous hydrogen.

2) Methane is adsorbed on surface Ni atoms. The adsorbed methane either reacts with the adsorbed oxygen or is dissociated to form chemisorbed radicals, such as $CH_3$-L, $CH_2$-L, CH-L and C-L.

3) The concentrations of the carbon containing radicals are much lower than the total concentration of the active sites.

4) The adsorbed oxygen and the carbon containing radicals react to form L-$CH_2O$, L-CHO, or L-CO, L-$CO_2$.

5) The hydrogen formed is directly released into the gas phase and/or the gaseous hydrogen is in equilibrium with H-L or $H_2$-L.

6) All the reaction schemes are thought to have a step for reactions 1, 2 and 3 with a rate potentially much slower than that of the other steps, so that it controls the overall reaction rate. It is the rate determining step.

Applying the Langmuir-Hinshelwood approach to the kinetic mechanisms, a set of different intrinsic rate equations can be derived as following.

$$r_1 = \frac{k_1}{P_{H_2}^{2.5}} \frac{\left(P_{CH_4} P_{H_2O} - P_{H_2}^3 P_{CO} / K_{e,1}\right)}{DEN^2} \quad (1)$$

$$r_2 = \frac{k_2}{P_{H_2}} \frac{\left(P_{CO} P_{H_2O} - P_{H_2} P_{CO_2} / K_{e,2}\right)}{DEN^2} \quad (2)$$

$$r_3 = \frac{k_3}{P_{H_2}^{3.5}} \frac{\left(P_{CH_4} P_{H_2O}^2 - P_{H_2}^4 P_{CO_2} / K_{e,3}\right)}{DEN^2} \quad (3)$$

where, $DEN = 1 + K_{CO} p_{CO} + K_{H2} p_{H2} + K_{CH4} p_{CH4} + K_{H2O} p_{H2O} / p_{H2}$ (4)

## *2. Equipment*

Experimental investigation on the kinetic analysis was conducted by micro reactor, and on the direct internal reforming performance verification was conducted by MCFC unit cell test station. A schematic diagram of the experimental equipment used is given in Fig. 1.

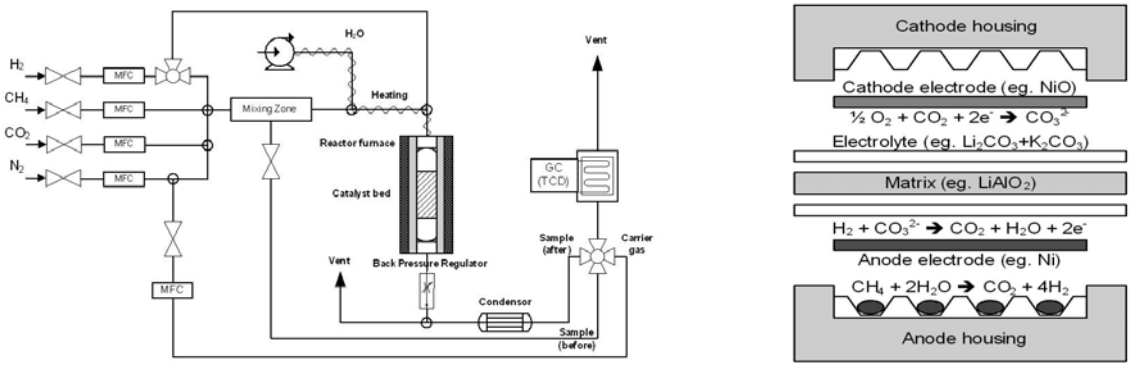


**(a)** **(b)**

**Fig. 1 Schematic diagram of experimental apparatus. (a : micro reactor, b : unit cell)**

The experimental equipments consist of feed section, reaction section and analysis section. The feed section contains gas and steam supplies. The flow rate of each gas was controlled by mass flow controller (MFC) at the desired value. The mixed gases flowed into the humidifier in which the gas mixture was heated. Deionised (DI) water was supplied by a high pressure liquid chromatography (HPLC) pump to the humidifier where it vaporized into steam and was mixed with the other gases in a predetermined steam to carbon ratio. The reaction section contains micro reactor and temperature controller. The micro reactor used in the present experiment was made from stainless steel tube enclosed by an electric resistance heater. A thermocouple located along the axis of the reactor was connected to a temperature indicator and a temperature controller to monitor and control the reaction temperature. The analysis section contains condenser and gas chromatograph (GC, Agilent 3000A).

On the other hand, the DIR-MCFC unit cell test was conducted to verify catalyst activity with real operating condition. The experimental equipment is similar to kinetic study equipment and schematic diagram of DIR-MCFC unit cell is given Fig. 1 (b).

### *3. Pre-treatment & Experiments*

A $Ni/Al_2O_3$ catalyst of extrusion type was used to this experiment. The physical properties of the catalyst are listed in Table 2. The original catalyst was crushed into particles of average diameter 0.1 mm to avoid intra-particle diffusion effects within present experimental conditions.

**Table 2. Catalyst properties**

| | | |
|---|---|---|
| Ni content | 48.9 | wt.% |
| Surface area (BET) | 236 | $m^2/g$ |
| Skeletal density | 2.28 | g/ml |
| Bulk density | 0.623 | g/ml |
| Pore volume | 0.61 | $cm^3/g$ |
| Pore size | 10.1 | Nm |
| Porosity | 72.7 | % |
| Ni metal dispersion | 7.2 | % |
| Ni metallic surface area | 25 | $m^2/g$ |
| NiO size | 2~4 | nm |

The catalyst contains about 45~50wt.% Ni which metal size is 2~4 nm and dispersion is 7.2%. An amount of catalyst loaded on reactor was 25mg ~ 100mg, which was mixed with alumina diluent in the 1~3 volume ratio.

The catalyst was reduced by the following procedure. First, the catalyst was heated to 773K at 4K/min in nitrogen and maintained at this temperature for 4 hrs. And then, it was heated to 923K at 2K/min and kept at this temperature for 4 hrs in hydrogen. After reduction process, the temperature was decreased to the required operating temperature in a stream of hydrogen and nitrogen. The initial activity of the catalyst drops rapidly during the first 24 hrs, but then much more gradually. So, the kinetic study of this work was started after 24 hrs on reactants stream.

On the other hand, a IR-MCFC unit cell consists of Ni anode electrode, $Li_2AlO_2$ matrix, NiO cathode electrode, $Li_2CO_3$-$K_2CO_3$ electrolyte and internal reforming catalyst. The powder catalyst was mixed with binder, plasticizer and solvent to make paste type. And then, it was loaded on anode gas channel as extrusion type. The pretreatment process of IR-MCFC is very complicated because of removing binders of unit cell components and activation the cell performance. When the unit cell temperature reached 650℃ after pretreatment process, the anode fuel gas was switched into $H_2$ or $CH_4$. The unit cell test of this work was conducted after 24 hrs due to unstable cell performance and reforming catalyst deactivation.

### *4. Results and Discussion*

Fig. 2 shows conversion curves of total methane conversion and conversion of methane into $CO_2$, vs. $W/F_{CH4}$ of steam reforming reaction for different temperatures.

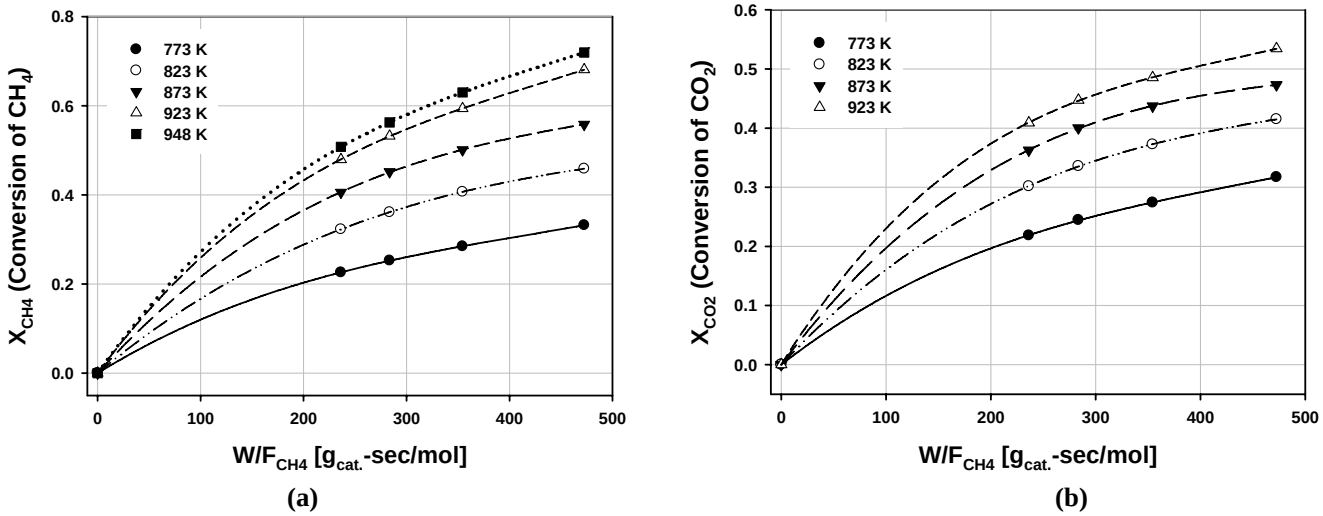


**(a)** **(b)**

**Fig. 2 Conversion of methane (a) and carbon dioxide (b) vs. contact time $W/F_{CH4}$ with S/C=3.14. (steam reforming).**

Similarly, the reverse-WGSR and methanation reaction results are presented Fig. 3.

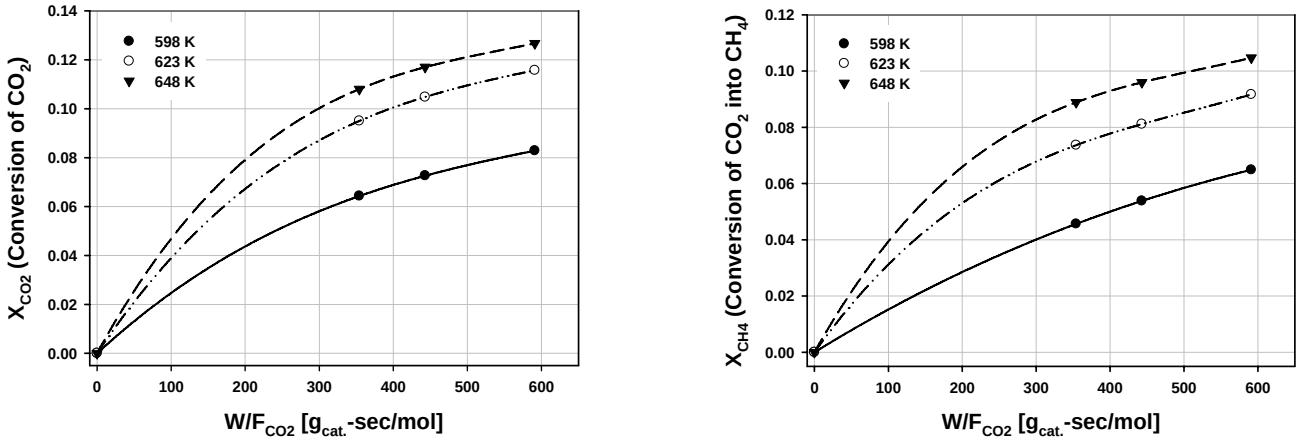


**Fig. 3 Conversion of carbon dioxide (a) into methane (b) vs. contact time $W/F_{CO2}$ with S/C=3.14. (reverse-WGSR)**

By differentiating equations of conversion, the methane disappearance rate and carbon dioxide formation rate can be given, respectively, as :

$$r_{CH4} = \frac{dX_{CH4}}{d(W/F_{CH4})} = a_1 + 2a_2\left(\frac{W}{F_{CH4}}\right) + 3a_3\left(\frac{W}{F_{CH4}}\right)^2 \quad (5)$$

$$r_{CO2} = \frac{dX_{CO2}}{d(W/F_{CO2})} = b_1 + 2b_2\left(\frac{W}{F_{CO2}}\right) + 3b_3\left(\frac{W}{F_{CO2}}\right)^2 \quad (6)$$

Similarly, applying to the reverse WGSR experiments, the carbon dioxide disappearance rate and methane formation rate can be obtained. And reaction rates for the formation carbon dioxide and for the disappearance of methane in steam reforming are predicted from:

$$r_{CO2} = r_2 + r_3 \quad (7), \quad r_{CH4} = r_1 + r_3 \quad (8)$$

The rate constants and adsorption parameters were estimated at each temperature by non-linear least square analysis were listed in Table 3.

**Table 3. Parameter estimates of kinetics model**

| Temp. (K) | $k_1 * 10^3$ | $k_2 * 10^3$ | $k_3 * 10^3$ | $K_{CO}$ | $K_{H2}$ | $K_{CH4}$ | $K_{H2O}$ |
|---|---|---|---|---|---|---|---|
| Steam Reforming | | | | | | | |
| 773 | 0.4971 | | 6.291 | | | 1.175E-01 | 8.178E-04 |
| 823 | 4.199 | | 22.13 | | | 4.335E-02 | 6.957E-03 |
| 873 | 0.2235 | | 0.9819 | | | 2.881E-05 | 5.180E-02 |
| 923 | 0.2646 | | 1.371 | | | 1.392E-04 | 2.356E-01 |
| Reverse of Water Gas Shift and Methanation reaction | | | | | | | |
| 598 | 0.03205 | 0.6751 | 0.0211 | 0.1317 | 0.9335 | | |
| 623 | 0.03952 | 0.2479 | 0.07163 | 0.4599 | 0.7068 | | |
| 648 | 0.2349 | 0.24 | 0.1328 | 0.1093 | 0.6217 | | |

These rate constants and adsorption parameters could be extended for all temperatures by the Arrhenius equation and the van't Hoff equation. Fig. 4 shows the temperature dependence of these parameters.

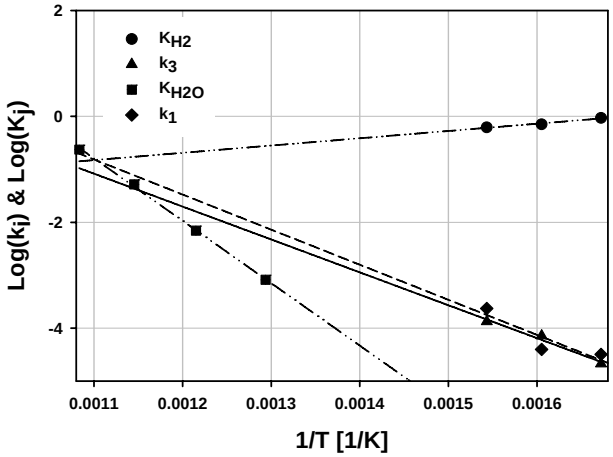


**Fig. 4 Temperature dependence of rate constants and adsorption parameters.**

By using the above kinetic equation data, we could decide the amount and loading pattern of the catalyst. Fig. 5 shows the IR-MCFC unit cell performance results of active area 100cm$^2$ (10cm * 10cm) vs. (a) : different fuel gas and (b) : utilization ratio of fuel.

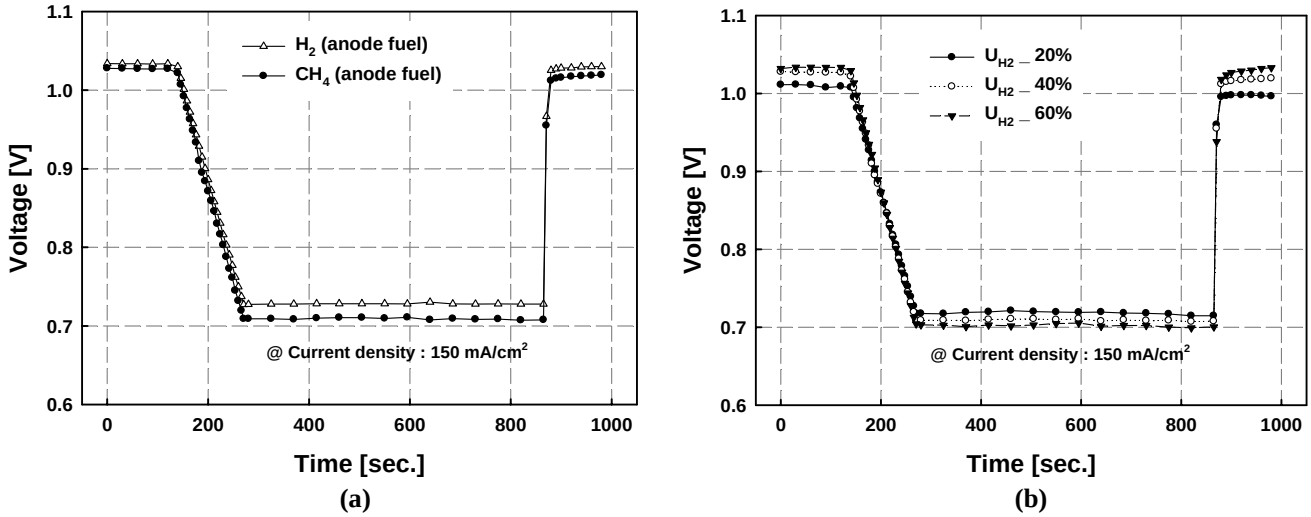


**Fig. 5 The IR-MCFC unit cell performance results. (a : various fuel, b : various $U_f$)**

The cell voltage with $CH_4$ anode fuel gas was lower than cell voltage with $H_2$ anode fuel gas as 6mV at no current and as 19mV at 150mA/cm$^2$ current density. But, it is very stable as $H_2$ fuel. It means that the internal reforming reaction produce $H_2$ well enough to satisfy the electrochemical reaction. Fig. 5 (b) shows the effect of anode fuel utilization on the cell voltage at 150mA/cm$^2$ current density. The difference of open circuit voltage (OCV) is larger than that of close circuit voltage (CCV). It means that the mole fractions of hydrogen for CCV are similar at various fuel utilization conditions, contrary to OCV results. The conversion of methane to hydrogen was increased at the CCV condition because the

steam reforming was promoted by electrochemical reaction as hydrogen removing reaction. It was verified by gas chromatography analysis data, the methane conversion is 82% at 0mA/$cm^2$ current density and 96% at 150mA/$cm^2$ current density.

## *5. Conclusions*

Based on the thermodynamic analysis, the kinetic rate equation for $Ni/Al_2O_3$ of the steam reforming catalyst has been obtained. The experiments of intrinsic kinetics were conducted separately for steam methane reforming and reverse water gas shift reaction. And the results were verified by internal reforming MCFC unit cell test. Applying this results and process with advanced simulation and modeling to stack, it will be possible to control of temperature distribution of IR-MCFC stack for long term operation.

## *References*


1. Kaihu Hou and Ronald Hughes (2001), "The kinetics of methane steam reforming over a Ni/a-Al2O catalyst," *Chemical Engineering Journal 82* pp.311-328.
2. Jianguo Xu and Gilbert F. Froment (1989), "Methane Steam Reforming, Methanation and Water-Gas Shift: I. Intrinsic Kinetics," *AIChE Journal 35(1)* pp. 88-96.
3. Toshinori Tsuru, Koji Yamaguchi, Tomohisa Yoshioka and Masashi Asaeda (2004) "Methane Steam Reforming by Microporous Catalytic Membrane Reactors," *AIChE Journal 50(11)* pp.2794-2805.
4. Stephen H. Clarke, Andrew L. Dicks, Kevin Pointon, Thomas A. Smith and Angie Swann (1997), "Catalytic aspects of the steam reforming of hydrocarbons in internal reforming fuel cells," *Catalysis Today 38* pp.411-423.
5. Chunshe Cao, Gordon Xia, Jamie Holladay, Evan Jones and Yong Wang (2004), "Kinetic studies of methanol steam reforming over Pd/ZnO catalyst using a microchannel reactor," *Applied Catalysis A: General 262* pp. 19-29.
6. L. M. Aparicio (1997), "Transient Isotopic Studies and Microkinetic Modeling of Methane Reforming over Nickel Catalysts," *Journal of Catalysis 165* pp. 262-274.
7. Kimihiko Sugiura, Mayumi Daimon, Kazumi Tanimoto (2003), "Optimum operating conditions of DIR-MCFC without vapor-phase carbonate pollution," *Journal of Power Sources 118* pp. 228-236.
8. Sanjay Patel, K. K. Pant (2007), "Experimental study and mechanistic kinetic modeling for selective production of hydrogen via catalytic steam reforming of methanol," *Chemical Engineering Science 62* pp. 5425-5435.
9. W. W. Akers and D. P. Camp (1955), "Kinetics of the Methane-steam Reaction," *AIChE Journal 1* pp. 471-475.
10. Mitsuie Matsumura and Chika Hirai (1998), "Deterioration Mechanism of Direct Internal Reforming catalyst," *Journal of Chemical Engineering of Japan 31* pp. 734-740.
11. J. R. Rostrup-Nielsen (1984), "Catalytic Steam Reforming," Springer, Berlin.
12. J. H. Park, J. S. Lee, H. C. Chung (1998), "Simulation on the Performance and Reaction of Direct Internal Reforming Molten Carbonate Fuel Cell (DIR-MCFC), " *Journal of the Korean Institute of Chemical Engineers* pp. 877-886.